Hydrogen sulfide produced during fermentation improves ethanol production in *Saccharomyces cerevisiae* an evolutionarily conserved effect in other yeast species

Emilio Espinoza-Simón[a*], Paola Moreno-Alvarez[a*], Emmanuel Ríos-Castro[b], Salvador Uribe-Carvajal[c], Francisco Torres-Quiroz[a#]

[a] División de Ciencia Básica, Departamento de Bioquímica y Biología Estructural, Instituto de Fisiología Celular, Universidad Nacional Autónoma de México (UNAM), Ciudad de México, México

[b] Unidad de Genómica, Proteómica y Metabolómica, LaNSE, Centro de Investigación y de Estudios Avanzados del I.P.N., Ciudad de México, México

[c] División de Ciencia Básica, Departamento de Genética Molecular, Instituto de Fisiología Celular, Universidad Nacional Autónoma de México (UNAM), Ciudad de México, México

*These authors contributed equally to this work

Address correspondence to Francisco Torres-Quiroz, ftq@ifc.unam.mx

Abstract

Hydrogen sulfide (H_2S) is a gas produced endogenously in organisms from the three domains of life. In mammals, it is involved diverse of physiological processes including regulation of blood pressure, and plays an important role in memory. In contrast, in unicellular organisms the physiological role of H_2S has not been studied in detail. In yeast, for example, in the winemaking industry H_2S is an undesirable byproduct because of its rotten egg smell, however its biological relevance has never been evaluated. The effect of H_2S in cells is linked to a post-translational

modification in cysteine residues known as S-persulfidation. We evaluated S-persulfidation in the *Saccharomyces cerevisiae* proteome. We screened S-persulfidated proteins from cells growing in fermentable carbon sources and we identified several glycolytic enzymes as S-persulfidation targets. Pyruvate kinase, catalyzing the last irreversible step of glycolysis, increases its activity in presence of a H_2S donor. Yeast cells treated with H_2S increased ethanol production; also, mutant cells that endogenously accumulate H_2S produced more ethanol and ATP during the exponential growth phase. This mechanism of regulation of metabolism seems to be evolutionarily conserved in other yeast species because H_2S induces ethanol production in the pre-Whole Genome Duplication *Kluyveromyces marxianus* and *Meyerozyma guilliermondii*. Our results suggest a new role of H_2S in regulation of metabolism that could be useful for biotechnological applications.

Introduction

Hydrogen sulfide (H_2S) is a gasotransmitter produced endogenously in cells. It has been associated with diverse physiological processes like vasodilation (1), pain (2) and longevity in animals (3), plant growth and development (4), bacterial antibiotic resistance (5), and as a byproduct of alcoholic fermentation in yeast (6). Surprisingly, the biological function of H_2S in yeast is not fully understood (7), the majority of reports describe how it is produced or how to prevent its production during fermentation (8–10). In yeast, the main metabolic pathway that produces H_2S is the sulfate assimilation pathway (11), where inorganic sulfate is transformed to H_2S and used in the synthesis of methionine and cysteine. This pathway is highly active in the exponential growth phase as sulfite reductase (6), the principal H_2S producer, is highly active. The synthesis of H_2S takes place in the

44 first hours of fermentation, and decreases at the final stages when cells reach the stationary phase
45 (12).

46 The molecular effect of hydrogen sulfide depends on a posttranslational modification named S-
47 persulfidation (originally termed sulfhydration) (13). S-persulfidation involves addition of a thiol
48 group to the cysteine residues (-S-SH) in proteins. This posttranslational modification has been
49 associated with the activation and inhibition of protein activity (13, 14).

50 In this work, we evaluated for the first time S-persulfidation of yeast proteins. We report that
51 hydrogen sulfide is a regulator of glycolysis that increases ethanol production in *S. cerevisiae*. This
52 was observed using an exogenous donor of hydrogen sulfide or mutant strains that accumulate or
53 produce less H_2S. This mechanism of regulation was conserved in pre-Whole Genome Duplication
54 (WGD) species, such as the thermotolerant *Kluyveromyces marxianus* from the KLE clade, and
55 the oleaginous yeast *Meyerozyma guilliermondii* from the CUG-Ser1 clade. This work provides
56 an insight on how H_2S regulates glucose metabolism through an evolutionarily conserved
57 mechanism, constituting an important role of H_2S in fermentation.

58

59 **Materials and methods**

60 ***Yeast strains, media, and growth conditions***

61 *Saccharomyces cerevisiae* strains used in this study were S288C-derived laboratory strains
62 BY4742 (*MATα his3Δ1 leu2Δ0 lys2Δ0 ura3Δ0*), BY4741 (*MATa his3Δ1 leu2Δ0 met15Δ0*
63 *ura3Δ0*). *Kluyveromyces marxianus* and *Meyerozyma guilliermondii* were isolated from mezcal
64 producers in Michoacán, México (15). Deletion strains derived from BY4742 were constructed by
65 PCR-based gene replacement using synthetic oligonucleotides and the kanMx and natMx

66 disruption modules contained in plasmids pUG6 and pAG25, strains and oligonucleotides are
67 listed in supplementary table 1. Strains were cultured at 30ºC in liquid YPD medium (1% yeast
68 extract, 2% dextrose, 2% peptone) or YPG medium (1% yeast extract, 2% galactose, 2% peptone)
69 until reaching the exponential growth phase (optical density at 660nm [OD_{660}] =0.5-0.6) and cells
70 were collected then for protein extraction.
71
72 ***Reagents***
73 Sodium hydrosulfide (NaHS), Methyl methanethiosulfonate (MMTS), dithiothreitol (DTT),
74 antibiotin antibody, neocuproine, deferoxamine and others chemicals were purchased from Sigma-
75 Aldrich, St Louis MO. N-(6-(biotinamido)hexyl)-3′-(2′-pyridyldithio)-propionamide (HPDP-
76 biotin), was obtained from Santa Cruz Biotechnology Dallas TX.
77
78 ***Modified biotin switch assay***
79 The modified biotin switch assay was performed as described previously (13;16). Briefly, after
80 yeast cultures reached exponential phase, cells were collected, and intracellular proteins were
81 extracted with chilled glass-beads in HEN buffer (250 mM HEPES-NaOH, 1 mM EDTA)
82 supplemented with 1% triton X-100, 0.1 mM neocuproine, 0.1 mM deferoxamine and 1X protease
83 cocktail inhibitor (Roche, Switzerland). Cell lysates were centrifuged at 14000 rpm for 1 hr at 4ºC,
84 total extracts (1-2 mg) were blocked in HEN buffer with 2.5% SDS and 20 mM MMTS at 50ºC
85 for 20 min. The MMTS was removed by acetone precipitation and the protein pellet was
86 resuspended in HEN buffer with 1% SDS. Protein labeling was performed with 0.8 mM HPDP-
87 biotin for 3 h at room temperature in the dark. The biotinylated proteins were separated by SDS-
88 polyacrylamide gel electrophoresis (PAGE) and subjected to immunoblot analysis.

89 ***Purification of biotinylated proteins***

90 After biotin switch assay, labeled extracts were subjected to streptavidin-based affinity
91 precipitation with magnetic beads. Labeled extracts were incubated with 3X volumes of
92 neutralization buffer (20 mM HEPES-NaOH pH 7.7, 100 mM NaCl, 1 mM EDTA, 0.5% triton)
93 and 25 µl of streptavidin magnetic beads (Pierce) with agitation, overnight at 4ºC. Magnetic beads
94 were collected and washed with wash buffer as indicated by manufacturer's instructions,
95 biotinylated proteins were eluted with IP-MS elution buffer and analyzed using LS-MS or SDS-
96 PAGE.

97

98 ***Immunoblot analysis***

99 Protein extracts were separated by SDS-PAGE and transferred to polyvinylidene difluoride
100 (PVDF) membranes (Millipore-Merck, Germany). Membranes were blocked with 5% non-fat milk
101 and incubated with a specific anti-biotin antibody overnight at 4ºC. Proteins were detected with
102 chemiluminescence using horse-radish peroxidase conjugated secondary antibodies (Jackson
103 ImmunoResearch, West Grove, PA). Before to immunoblot, membranes were stained using
104 Ponceau red (Millipore-Merck, Germany) as protein loading control.

105

106 ***Quantification of intracellular ATP concentration***

107 NaHS was added to cells cultures at specific timepoints, then cells were centrifuged, and
108 intracellular ATP was measured using the ATP Bioluminescent Assay Kit HS II (Roche,
109 Switzerland). Cell samples were prepared by diluting treated cells to a final concentration of
110 $3.7x10^9$ cells·ml^{-1} in 500 µl with a buffer containing 100 mM Tris-HCl pH 7.8 and 4 mM EDTA.
111 After 2 min incubation, samples were immersed in boiling water for 2 minutes, and the resulting

112 cell extracts were incubated for 5 minutes at 4ºC, cell debris were removed by centrifugation at
113 14000 rpm for 5 min and supernatants were used to measure the amount of intracellular ATP using
114 an ATP calibration curve prepared each time, as indicated by the manufacturer. Bioluminescence
115 was detected in a POLARstar Omega luminometer (BGM LABTECH, Offenburg, Germany).
116
117 ***Detection of H_2S production***
118 H_2S production by yeast strains colonies was detected through the generation of a visible black
119 precipitate indicating that the hydrogen sulfide gas has reacted with lead nitrate (17). Yeast strains
120 were diluted, and cell density normalized to $3x10^7$ cells/ml. Cells were spotted in solid media
121 (3.2% dextrose, 0.4% yeast extract, 0.24% peptone, 0.016% ammonium sulfate, 0.08% lead
122 nitrate, 1.6% agar) and plates were kept at 30ºC for 5-7 days.
123
124 ***Fermentation assays***
125 BY4742 *wt* and derived mutants were grown in YPD media under temperature-controlled
126 conditions. Cells precultured under agitation for 24h at 30ºC, were inoculated in fresh media with
127 an initial DO_{660}=0.2. When cells reached DO_{660}=0.5, a pulse of NaHS was added. After 7h of
128 NaHS addition, aliquots of 2 ml were obtained, DO_{660} was measured and cells centrifuged at 14000
129 rpm for 1 min. Supernatants were stored at -20ºC for subsequent ethanol quantification. For mutant
130 and *wt* strains, aliquots were taken every hour after cells were inoculated, supernatants were stored
131 at -20ºC. Ethanol production was evaluated through enzymatic activity of alcohol dehydrogenase
132 (ADH), that oxidize ethanol to acetaldehyde using NAD^+ as cofactor and subsequently reducing it
133 to form NADH. Supernatants were incubated in buffer (114 mM K_2HPO_4 pH7.6), 1.8 mM NAD^+,

134 39 μg·mL^{-1} ADH for 30 min at 30ºC with vigorous agitation (18). Produced NADH was monitored
135 by the increase in absorbance at 340 nm. The results are reported as mM ethanol per 1x10^{7} cells.
136

137 ***Enzymes activity assays***

138 GAPDH (13), pyruvate kinase (PK) (19) and alcohol dehydrogenase (ADH) (20) activities were
139 measured by specific reaction assays and monitored spectrophotometrically at 340 nm, recording
140 the rate of NAD to NADH reduction. Cells cultures were exposed to NaHS at different times,
141 protein extracts were quantified and 10 μg of protein were incubated in assay buffer as follows:
142 for GAPDH (20 mM Tris-HCl pH7.8, 100 mM NaCl, 0.1 mg·mL^{-1} BSA, 2 mM NAD^{+}, 10 mM
143 sodium pyrophosphate, 20 mM sodium arsenate, 500 mM DTT buffer, PBS 1X, 27.3 mM
144 glyceraldehyde 3-phosphate [G3P]). For PK (50 mM Imidazole·HCl, 120 mM KCl, 62 mM
145 $MgSO_4$ pH7.6, 45 mM ADP, 6.6 mM NADH, 45 mM phosphoenolpyruvate [PEP], 1.3 KU·mL^{-1}
146 LDH). For ADH (114 mM K_2HPO_4 pH7.6), 1.8 mM NAD^{+}, 39 μg·mL^{-1} ADH, 16.4 mM ethanol).
147

148 ***Sample preparation and LC-MALDI-MS/MS***

149 Biotinylated proteins were digested with 250 ng of trypsin mass spectrometry grade (Sigma-
150 Aldrich, St. Louis, MO) in 50 mM of ammonium bicarbonate (ABC). Resulting tryptic peptides
151 were desalted using ZipTip C18 (Millipore) and concentrated to an approximated volume of 10
152 μL. Afterward, 9 μL were loaded into ChromXP Trap Column C18-CL precolumn (Eksigent,
153 Redwood City CA); 350 μm X 0.5 mm, 120 Aº pore size, 3 μm particle size and desalted with
154 0.1% TFA in H_2O at a flow of 5 μL min^{-1} for 10 min. Then, peptides were loaded and separated
155 on a 3C18-CL-120 column (Eksigent, Redwood City CA); 75 μm X 150 mm, 120 Aº pore size, 3
156 μm particle size, in a HPLC Ekspert nanoLC 425 (Eksigent, Redwood City CA) using as a mobile

157 phase A, 0.1% TFA in H_2O and mobile phase B 0.1% TFA in ACN under the following lineal
158 gradient: 0-3 min 10% B, 60 min 60% B, 61-64 min 90 % B, 65 to 90 min 10% B at a flow of 250
159 nL min^{-1}. Eluted fractions were automatically mixed with a solution of 2 $mg \cdot mL^{-1}$ of CHCA in
160 0.1%TFA and 50% ACN as a matrix, spotted in an Opti-TOF plate of 384 spots using a MALDI
161 Ekspot (Eksigent, Redwood City CA) with a spotting velocity of 20 s per spot at a matrix flow of
162 1.6 μL min^{-1}. The generated spots were analyzed by a MALDI-TOF/TOF 4800 Plus mass
163 spectrometer (ABSciex, Framingham MA). Each MS Spectrum was acquired by an accumulation
164 of 1000 shots in a mass range of 850-4000 Th with a laser intensity of 3800. The 100 more intense
165 ions with a minimum signal-noise (S/N) of 20 were programmed to fragmenting. The MS/MS
166 spectra were obtained by fragmentation of selected precursor ions using Collision-Induced
167 Dissociation (CID) and acquired by 3000 shots with a laser intensity of 4300. Generated MS/MS
168 spectrums were compared using Protein Pilot software v. 2.0.1 (ABSciex, Framingham MA)
169 against *Saccharomyces cerevisiae,* strain ATCC 204508/S288c database (downloaded from
170 Uniprot, 6049 protein sequences) using Paragon algorithm. Search parameters were: Not constant
171 modifications in cysteines, trypsin as a cutter enzyme, all the biological modifications and amino
172 acids substitution set by the algorithm (including carbamidomethylated cysteine as a variable
173 modification); as well as phosphorylation emphasis and Gel-based ID as special factors. The
174 detection threshold was considered in 1.3 to acquire 95% of confidence; additionally, the identified
175 proteins showed a local FDR of 5% or less. Identified proteins were grouped by ProGroup
176 algorithm in the software to minimize redundancy.

177

178

179 **Results**

180 **S-Persulfidation of yeast proteins growing on a fermentable carbon source.**

181 Protein S-persulfidation was detected using the modified biotin switch method (21). In order to
182 validate the method in yeast, we performed the assay in either a poor producer (*met5*Δ*met10*Δ) or
183 an accumulator (*met17*Δ) strain of H_2S and compared them to the *wt* (Figure 1A). Cells grew using
184 glucose as carbon source and at exponential phase, when H_2S is produced (6), protein was
185 extracted. S-Persulfidated proteins are accumulated in *met17*Δ in comparison to *met5met10*Δ strain
186 and *wt* as expected (Figure 1B).

187 In yeast, H_2S is produced during fermentation, however S-persulfidation target proteins are not
188 known. We decided to analyze by mass spectrometry the S-persulfidated proteins in cells growing
189 at exponential phase in two different fermentable carbon sources: glucose and galactose. Glucose
190 is the preferred fermentable carbon source of yeast, while galactose needs to be isomerized to enter
191 to the glycolytic pathway. We found 42 S-persulfidated proteins, 21 were specific to glucose-
192 grown cells, 4 specific to galactose-grown cells, and 17 proteins were found in both conditions
193 (Supplementary Table 2). Among the generally expressed 17 proteins, 15 where reported before
194 as proteins with a redo- regulated cysteine (22), which is a feature of cysteines susceptible of post-
195 translational modifications (21). Cytoplasmic translation (7 proteins) and glycolysis (7 proteins)
196 where the biological processes the most represented in cells growing in either condition.
197 Interestingly, Pdc1, a key enzyme in alcoholic fermentation, and Adh1-the major enzyme
198 responsible of ethanol synthesis- were also found, suggesting a possible role of S-persulfidation in
199 fermentation. The identity of some glycolytic enzymes GAPDH, enolase and triosephosphate
200 isomerase (Tdh3, Eno2 and Tpi1, respectively) was confirmed using specific antibodies (Figure

201 2). We also tested cystathionine beta-synthase (Cys4), which was described before as a possible
202 S-persulfidated protein (13, 23) and even if it must be considered that in our mass spectrometry
203 analysis it did not pass the threshold (unused score of 1.04, coverage of 43.98%), we did find that
204 Cys4 is a target of S-persulfidation.

205

206 **H_2S increases glycolytic enzymes activities**

207 Among the first effects of S-persulfidation described is the increase of GAPDH activity (13).
208 Considering that Tdh3 (GAPDH) was one of the glycolytic enzymes targeted for S-persulfidation,
209 we decided to test the effect of NaHS (a donor of H_2S) on GAPDH activity. Cells were stimulated
210 with 0.1 mM or 0.25 mM NaHS for two and seven hours. Then, protein was extracted and GAPDH
211 activity was measured. We found that after two hours of stimulation NaHS both at 0.1 mM and
212 0.25 mM increase GAPDH activity 1.4 times (Figure 3A) and the effect was lost at seven hours
213 (Figure 3B). Another protein identified by mass spectrometry was pyruvate kinase (PK) that
214 catalyzes the last irreversible step of glycolysis. We measured the activity of the pyruvate kinase
215 at two hours of treatment with 0.1 mM or 0.25 mM NaHS finding that NaHS increased PK activity
216 2.39 times (Figure 3C, Supplementary Table 3). Finally, we subjected alcohol dehydrogenase
217 (ADH) to the same treatment and we did not find any significant difference between the treated
218 and untreated cells, i.e., at these concentrations NaHS did not affected ADH activity (Supplemental
219 Figure 1).

220

221

222 **H_2S stimulates fermentation**

223 The glycolytic enzymes GAPDH and PK increased their activity in response to H_2S. In addition,
224 mass spectrometry data indicated that these and other enzymes from glycolysis where S-
225 persulfidated. Thus, we decided to test if H_2S has an effect on synthesis of ethanol. Exponential-
226 phase grown cells were treated with 0.1 mM NaHS and after seven hours, the supernatant was
227 collected. It was observed that treated cells increased ethanol production as compared to the control
228 (Figure 4A).

229 In order to test the effect of endogenous H_2S in fermentation, we decided to compare ethanol
230 production in the two isogenic lab strains BY4741 and BY4742. The only difference between these
231 two strains is that BY4741 has a deletion of *MET17* and strain BY4742 has a deletion of *LYS2*. As
232 mentioned before a *met17*Δ strain accumulates endogenously H_2S because *MET17* codifies for the
233 enzyme using H_2S and O-acetyl homoserine to synthetize homocysteine. An overnight preculture
234 of each strain was diluted to an OD_{600}=0.2, supernatants were collected 24 h after, and ethanol was
235 quantified. The strain accumulating H_2S endogenously, BY4741 *met17*Δ, produced more ethanol
236 than the strain BY4742 *MET17* (Figure 4B).

237 Ethanol is the main product of fermentation. Additionally, during glycolytic fermentation two ATP
238 molecules are synthesized. Thus, we decided to quantify the ATP after the treatment with NaHS.
239 Exponential-phase cells were treated with the same quantities of NaHS used before and ATP was
240 quantified two and four hours after treatment. After two hours, treated cells produced more ATP
241 than the untreated cells; this effect was lost four hours after treatment (Figure 4C). These results
242 suggest that H_2S stimulates glycolysis and that fermentation is enhanced to produce both ATP and
243 ethanol.

244 Based on these results we decided to compare if the endogenous H_2S has an influence on the onset
245 of ethanol synthesis. We measured the ethanol production in 48 hours precultures of the poor H_2S
246 producer strain *met5*Δ*met10*Δ, the H_2S accumulator *met17*Δ strain, and the *wt*. Cells from a 48
247 hours preculture were resuspended in fresh media and aliquots from the supernatant were collected
248 every hour. Strain *met17*Δ strain initiated ethanol production at five hours, *wt* strain at six hours
249 and *met5*Δ*met10*Δ after seven hours, respectively (Figure 5A). This result shows that cells with
250 high endogenously accumulated H_2S began ethanol production before than the cells with lower
251 H_2S concentration.

252 Finally, in each of these strains we quantified the ATP at exponential or stationary phase. We
253 found that the endogenously H_2S accumulator strain produced the most ATP at exponential phase,
254 wile no differences in the ATP concentration at the stationary phase between the *wt* and mutant
255 strains (Figure 5B). These results support our proposal that H_2S stimulates ethanol and ATP
256 production.

257

258 **H_2S stimulates ethanol production in *Meyerozyma guilliermondii* and *Kluyveromyces***
259 ***marxianus*.**

260 Ethanol synthesis is more robust in Crabtree positive yeast species, this phenomenon is associated
261 with the WGD (24). Evidence suggests that the WGD event arose from an interspecies
262 hybridization between a strain from the KLE clade (genera Kluyveromyces, Lachancea and
263 Eremothecium) and a strain from the ZT clade (Zygosaccharomyces and Torulaspora) (25). The
264 CUG-Ser1 clade first appeared approximately 117 million years before the WGD event; the CUG-
265 Ser1 clade is characterized by a change in codon usage (26). Considering this, we decided to test

266 the effect of H_2S during ethanol synthesis on the KLE clade strain, *K. marxianus* and in *M.*
267 *guilliermondii* from the CUG-Ser1 clade. *K. marxianus* exponential-phase cells were stimulated
268 with NaHS. Treatment with the H_2S donor in *K. marxianus* increased ethanol synthesis as in *S.*
269 *cerevisiae* (Figure 5a). In *M. guilliermondii,* it was noted that ethanol synthesis takes longer than
270 24 h when glucose is the carbon source (27), for this reason exponential-phase cells were treated
271 with NaHS and treated again 24 h later. As observed in *K. marxianus*, ethanol synthesis increased
272 after the H_2S donor treatment on *M. guilliermondii* (Figure 5b) confirming that there is an effect
273 of H_2S on the fermentation activity of these two species of yeast.

274

275 **Discussion**

276 Hydrogen sulfide is produced endogenously in yeast and it is considered a fermentation byproduct,
277 however its biological role is unknown. The biological effects of H_2S are linked to a cysteine
278 posttranslational modification termed S-persulfidation (13). In this work, we analyzed S-
279 persulfidated proteins on the yeast proteome. We identified several glycolytic enzymes as S-
280 persulfidation targets, as reported previously in tissues such as brain, heart and liver (23), in
281 hepatocytes (13), a pancreatic beta cell line (28), HEK293 cells (23), plant (29, 30) and bacteria
282 (31). Interestingly, Fu and collaborators reported six S-persulfidated glycolytic enzymes
283 (ALDOA, GAPDH, PGK1, ENO1, PKM and LDHA) when they evaluated S-persulfidated
284 proteins in cells overexpressing the H_2S producer enzyme cystathionine gamma-lyase (CSE) (23).
285 In a previous report in pancreatic beta cells, metabolites were measured and H_2S was associated
286 to an increased glycolytic metabolic flux of cells under a chronic stress. Curiously, all these reports
287 agreed that several glycolytic enzymes are S-persulfidated, even when the activity of GAPDH is

288 the only one that has been measured (13). In *S. cerevisiae*, we found that GAPDH increases its
289 activity with the H_2S donor NaHS two hours after the treatment, and the effect is lost at seven
290 hours. It is important to note that H_2S is released from NaHS just a few seconds after the sodium
291 salt is dissolved (32), hence the effect of NaHS two hours after treatment may be attributed to a
292 chemical modification on the enzymes such as S-persulfidation. The thioredoxin system eliminates
293 this post-translational modification (33, 34), which is consistent with the idea that cellular
294 mechanisms maintain protein S-persulfidation homeostasis (35). Seven hours after stimulation
295 there is no effect on GAPDH activity probably due to loss of S-persulfidation by the protein.
296 Furthermore, the cells are no longer at an exponential phase seven hours after the OD_{600} reaches
297 0.5 and yeast metabolism changes to aerobic at the diauxic shift. Enzymes catalyzing the
298 irreversible steps regulates the glycolytic pathway (36); and we found that the enzyme involved in
299 the last irreversible step –pyruvate kinase– increases its activity when stimulated with NaHS. The
300 increase in pyruvate kinase activity may have at least two important consequences: feeding the
301 Krebs cycle and/or stimulating synthesis of ethanol. Considering that yeast synthetizes H_2S during
302 fermentation, we decided to test if NaHS increases ethanol production. We found that cells treated
303 with H_2S donor produce more ethanol. In order to confirm our observations, we measured the
304 ethanol production in the isogenic strains BY4741 and BY4742. These strains have almost the
305 same selection markers and they differ only in one of them, BY4741 accumulates H_2S because is
306 *met17*Δ and BY4742 is *lys2*Δ, and thus it does not accumulate H_2S. We observed that BY4741
307 produces more ethanol than BY4742, suggesting that endogenous H_2S levels increase ethanol
308 synthesis. Previously, it was reported that BY4742 fermenting activity is slower than in BY4741;
309 it would be very interesting to analyze the role of H_2S in this system (37). Considering these results,
310 we proposed that if H_2S stimulates fermentation, then mutants accumulating H_2S would begin

311 ethanol production before strains producing less H_2S. We tested this hypothesis by comparing
312 ethanol production between the lesser producer of H_2S strain *met5*Δ*met10*Δ, the accumulator strain
313 *met17*Δ and the *wt*. We found that *met17*Δ strain starts producing ethanol before the *wt* strain, and
314 in turn the *met5*Δ*met10*Δ strain production of ethanol is delayed even longer. Results confirmed
315 that endogenous concentrations of H_2S affects ethanol synthesis. Finally, we measured ATP
316 production in all strains, and we found that at logarithmic phase the *met17*Δ strain produces more
317 ATP than the others. This result supports the idea that in addition to increasing an early synthesis
318 of ethanol, H_2S and also enhances ATP production at the exponential phase of growth.

319 It is accepted that the origin of *S. cerevisiae* comes from a WGD event, probably by the interspecies
320 hybridization between a strain from the KLE clade and a strain from the ZT clade (33). WGD
321 species have a more pronounced Crabtree effect that non-WGD species (24), so we decided to test
322 if H_2S has an effect on yeast from the parental KLE clade that originated *S. cerevisiae* and a
323 Crabtree-negative species from the CUG-Ser1 clade. The origin of this clade is estimated between
324 178 and 248 million years ago (mya), and this event occurred before WGD, estimated between 82
325 and 105 mya (26). We found that both species increase ethanol production after the NaHS
326 treatment suggesting that i) H_2S is a positive regulator of fermentation and ii) this effect is
327 evolutionarily conserved.

328 Overall, H_2S is considered as a fermentation byproduct on yeast even when its biological effect is
329 unknown. Here, we proposed a very different picture that will change our vision of how H_2S
330 regulates cell metabolism. Ethanol synthesis occupies a central position in the wine and beer
331 industry and it is a renewable energy source when used as bioethanol. In fact, that we found that
332 H_2S stimulates ethanol synthesis suggesting that the use of H_2S donors could be desirable for
333 industrial applications such as the biotechnology of biofuels production. In conclusion, our data

334 demonstrated that H_2S is a regulator of energetic metabolism. These results fill a major gap in the
335 understanding of H_2S and its control of ethanol production, which is evolutionarily conserved
336 among yeast species. Finally, our work provides the foundation for a mechanistic understanding
337 of the effects of H_2S.

338

339 **Acknowledgments**

340 This work was supported by the Programa de Apoyo a Proyectos de Investigación e Innovación
341 Tecnológica from the Dirección General de Asuntos del Personal Academico of the Universidad
342 Nacional Autonoma de Mexico (FTQ: UNAM-DGAPA-PAPIIT IA200315, IA202217 and
343 IN209219; SUC: IN208821) and from the Consejo Nacional de Ciencia y Tecnología,
344 Convocatoria de Ciencia Básica to FTQ (CONACyT-CB-238681).

345

346 Authors acknowledge Dr. Antonio Peña and Dr. Norma Silvia Sanchez for the *Kluyveromyces*
347 *marxianus* and *Meyerozyma guilliermondii* strains provided and Dr. Natalia Chiquete-Félix for
348 technical assistance.

349

350 **References**

351 1. Yang G, Wu L, Jiang B, Yang W, Qi J, Cao K, Meng Q, Mustafa AK, Mu W, Zhang S,
352 Snyder SH, Wang R. 2008. H2S as a physiologic vasorelaxant: hypertension in mice with
353 deletion of cystathionine gamma-lyase. Science 322:587–590.

354 2. Kawabata A, Ishiki T, Nagasawa K, Yoshida S, Maeda Y, Takahashi T, Sekiguchi F, Wada
355 T, Ichida S, Nishikawa H. 2007. Hydrogen sulfide as a novel nociceptive messenger. Pain
356 132:74–81.

357 3. Hine C, Harputlugil E, Zhang Y, Ruckenstuhl C, Lee BC, Brace L, Longchamp A, Treviño-
358 Villarreal JH, Mejia P, Ozaki CK, Wang R, Gladyshev VN, Madeo F, Mair WB, Mitchell
359 JR. 2015. Endogenous hydrogen sulfide production is essential for dietary restriction
360 benefits. Cell 160:132–144.

361 4. Dooley FD, Nair SP, Ward PD. 2013. Increased growth and germination success in plants
362 following hydrogen sulfide administration. PLoS One 8:e62048.

363 5. Shatalin K, Shatalina E, Mironov A, Nudler E. 2011. H2S: a universal defense against
364 antibiotics in bacteria. Science 334:986–990.

365 6. Jiranek V, Langridge P, Henschke PA. 1995. Regulation of hydrogen sulfide liberation in
366 wine-producing Saccharomyces cerevisiae strains by assimilable nitrogen. Appl Environ
367 Microbiol 61:461–467.

368 7. Huang C-W, Walker ME, Fedrizzi B, Gardner RC, Jiranek V. 2017. Hydrogen sulfide and its
369 roles in Saccharomyces cerevisiae in a winemaking context. FEMS Yeast Res 17.

370 8. Huang C, Roncoroni M, Gardner RC. 2014. MET2 affects production of hydrogen sulfide
371 during wine fermentation. Appl Microbiol Biotechnol 98:7125–7135.

372 9. Boudreau TF, Peck GM, O'Keefe SF, Stewart AC. 2017. The interactive effect of fungicide
373 residues and yeast assimilable nitrogen on fermentation kinetics and hydrogen sulfide
374 production during cider fermentation. J Sci Food Agric 97:693–704.

375 10. Wang C, Liu M, Li Y, Zhang Y, Yao M, Qin Y, Liu Y. 2018. Hydrogen sulfide synthesis in
376 native Saccharomyces cerevisiae strains during alcoholic fermentations. Food Microbiol
377 70:206–213.

378 11. Mendoza-Cózatl D, Loza-Tavera H, Hernández-Navarro A, Moreno-Sánchez R. 2005. Sulfur
379 assimilation and glutathione metabolism under cadmium stress in yeast, protists and plants.
380 FEMS Microbiol Rev 29:653–671.

381 12. Oka K, Hayashi T, Matsumoto N, Yanase H. 2008. Decrease in hydrogen sulfide content
382 during the final stage of beer fermentation due to involvement of yeast and not carbon
383 dioxide gas purging. J Biosci Bioeng 106:253–257.

384 13. Mustafa AK, Gadalla MM, Sen N, Kim S, Mu W, Gazi SK, Barrow RK, Yang G, Wang R,
385 Snyder SH. 2009. H2S signals through protein S-sulfhydration. Sci Signal 2:ra72.

386 14. Krishnan N, Fu C, Pappin DJ, Tonks NK. 2011. H2S-Induced sulfhydration of the
387 phosphatase PTP1B and its role in the endoplasmic reticulum stress response. Sci Signal
388 4:ra86.

389 15. Estrada-Ávila AK, González-Hernández JC, Calahorra M, Sánchez NS, Peña A. 2022.
390 Xylose and yeasts: A story beyond xylitol production. Biochim Biophys Acta Gen Subj
391 1866:130154.

392 16. Paul BD, Snyder SH. 2015. Protein sulfhydration. Methods Enzymol 555:79–90.

393 17. Cost GJ, Boeke JD. 1996. A useful colony colour phenotype associated with the yeast
394 selectable/counter-selectable marker MET15. Yeast 12:939–941.

395 18. Peña A, Sánchez NS, González-López O, Calahorra M. 2015. Mechanisms involved in the
396 inhibition of glycolysis by cyanide and antimycin A in Candida albicans and its reversal by
397 hydrogen peroxide. A common feature in Candida species. FEMS Yeast Res 15:fov083.

398 19. Sakai H, Suzuki K, Imahori K. 1986. Purification and properties of pyruvate kinase from
399 Bacillus stearothermophilus. J Biochem 99:1157–1167.

400 20. Bergmeyer HV, Gawhn K, Grassel M. 1974. Alcohol dehydrogenase, p. 428–429. *In*
401 Methods of Enzymatic Analysis, 2nd ed. Academic Press, New York.

402 21. Alcock LJ, Perkins MV, Chalker JM. 2018. Chemical methods for mapping cysteine
403 oxidation. Chem Soc Rev 47:231–268.

404 22. Marino SM, Li Y, Fomenko DE, Agisheva N, Cerny RL, Gladyshev VN. 2010.
405 Characterization of surface-exposed reactive cysteine residues in Saccharomyces cerevisiae.
406 Biochemistry 49:7709–7721.

407 23. Fu L, Liu K, He J, Tian C, Yu X, Yang J. 2020. Direct Proteomic Mapping of Cysteine
408 Persulfidation. Antioxid Redox Signal 33:1061–1076.

409 24. Dashko S, Zhou N, Compagno C, Piškur J. 2014. Why, when, and how did yeast evolve
410 alcoholic fermentation? FEMS Yeast Res 14:826–832.

411 25. Marcet-Houben M, Gabaldón T. 2015. Beyond the Whole-Genome Duplication:
412 Phylogenetic Evidence for an Ancient Interspecies Hybridization in the Baker's Yeast
413 Lineage. PLoS Biol 13:e1002220.

414 26. Shen X-X, Opulente DA, Kominek J, Zhou X, Steenwyk JL, Buh KV, Haase MAB,
415 Wisecaver JH, Wang M, Doering DT, Boudouris JT, Schneider RM, Langdon QK, Ohkuma
416 M, Endoh R, Takashima M, Manabe R-I, Čadež N, Libkind D, Rosa CA, DeVirgilio J,
417 Hulfachor AB, Groenewald M, Kurtzman CP, Hittinger CT, Rokas A. 2018. Tempo and
418 Mode of Genome Evolution in the Budding Yeast Subphylum. Cell 175:1533-1545.e20.

419 27. Fabricio MF, Valente P, Záchia Ayub MA. 2019. Oleaginous yeast Meyerozyma
420 guilliermondii shows fermentative metabolism of sugars in the biosynthesis of ethanol and
421 converts raw glycerol and cheese whey permeate into polyunsaturated fatty acids. Biotechnol
422 Prog 35:e2895.

423 28. Gao X-H, Krokowski D, Guan B-J, Bederman I, Majumder M, Parisien M, Diatchenko L,
424 Kabil O, Willard B, Banerjee R, Wang B, Bebek G, Evans CR, Fox PL, Gerson SL, Hoppel
425 CL, Liu M, Arvan P, Hatzoglou M. 2015. Quantitative H2S-mediated protein sulfhydration
426 reveals metabolic reprogramming during the integrated stress response. Elife 4:e10067.

427 29. Aroca Á, Serna A, Gotor C, Romero LC. 2015. S-sulfhydration: a cysteine posttranslational
428 modification in plant systems. Plant Physiol 168:334–342.

429 30. Aroca A, Benito JM, Gotor C, Romero LC. 2017. Persulfidation proteome reveals the
430 regulation of protein function by hydrogen sulfide in diverse biological processes in
431 Arabidopsis. J Exp Bot 68:4915–4927.

432 31. Peng H, Zhang Y, Palmer LD, Kehl-Fie TE, Skaar EP, Trinidad JC, Giedroc DP. 2017.
433 Hydrogen Sulfide and Reactive Sulfur Species Impact Proteome S-Sulfhydration and Global
434 Virulence Regulation in Staphylococcus aureus. ACS Infect Dis 3:744–755.

435 32. Li L, Whiteman M, Guan YY, Neo KL, Cheng Y, Lee SW, Zhao Y, Baskar R, Tan C-H,
436 Moore PK. 2008. Characterization of a novel, water-soluble hydrogen sulfide-releasing
437 molecule (GYY4137): new insights into the biology of hydrogen sulfide. Circulation
438 117:2351–2360.

439 33. Ju Y, Wu L, Yang G. 2016. Thioredoxin 1 regulation of protein S-desulfhydration. Biochem
440 Biophys Rep 5:27–34.

441 34. Wedmann R, Onderka C, Wei S, Szijártó IA, Miljkovic JL, Mitrovic A, Lange M, Savitsky
442 S, Yadav PK, Torregrossa R, Harrer EG, Harrer T, Ishii I, Gollasch M, Wood ME, Galardon
443 E, Xian M, Whiteman M, Banerjee R, Filipovic MR. 2016. Improved tag-switch method
444 reveals that thioredoxin acts as depersulfidase and controls the intracellular levels of protein
445 persulfidation. Chem Sci 7:3414–3426.

446 35. Paul BD, Filipovic MR. 2021. Editorial: Molecular Mechanisms of Thiol-Based Redox
447 Homeostasis and Signaling in the Brain. Front Aging Neurosci 13:771877.

448 36. Campbell-Burk SL, Shulman RG. 1987. High-resolution NMR studies of Saccharomyces
449 cerevisiae. Annu Rev Microbiol 41:595–616.

450 37. Harsch MJ, Lee SA, Goddard MR, Gardner RC. 2010. Optimized fermentation of grape juice
451 by laboratory strains of Saccharomyces cerevisiae. FEMS Yeast Res 10:72–82.

452 38. Wolfe KH. 2015. Origin of the Yeast Whole-Genome Duplication. PLoS Biol 13:e1002221.

453

454

455

456

457

458 **Figure Legends**

459 **Figure 1. H_2S productivity correlates with S-persulfidated proteins levels.** (A) H_2S
460 productivity by *wt*, *met5*Δ*met10*Δ and *met17*Δ. Cells were incubated at 30°C on YPDL plates for
461 4 days. (B) S-persulfidated proteins in *wt*, *met5*Δ*met10*Δ and *met17*Δ strains. Whole cell extracts
462 from exponential phase cultures were subjected to the modified biotin switch assay with antibody
463 against biotin (α-Biotin Ab) to detect S-persulfidation.

464

465 **Figure 2. Confirmation of S-persulfidated proteins by streptavidin beads precipitation.**
466 Whole cell extracts from exponential phase cultures were subjected to the modified biotin switch
467 assay, precipitated with streptavidin beads and detected with antibodies specific to each protein
468 Eno2, Tdh3, Cys4 and Tpi1. HPDP-B: (N-[6-(biotinamido)hexyl]-3'-(2'-
469 pyridyldithio)propionamide), TCL: Total cell lysate, PP STREP: Streptavidin precipitation.

470

471 **Figure 3. H_2S increase the activity of GAPDH and Pyruvate Kinase two hours after**
472 **stimulation**. (A) Yeast cell cultures at exponential phase were treated with NaHS 0.1 and 0.25
473 mM. Two hours later whole cell extracts were used to measure GAPDH activity *in vitro* at 37°C.
474 One-way ANOVA ** $P<0.0001$. (B) Yeast cell cultures at exponential phase were treated with
475 NaHS 0.1 and 0.25 mM. Seven hours later whole cell extracts were used to measure GAPDH
476 activity *in vitro* at 37°C. (C) Yeast cell cultures at exponential phase were treated with NaHS 0.1
477 and 0.25 mM. Two hours later whole cell extracts were used to measure Pyruvate Kinase activity
478 *in vitro* at 37°C. One-way ANOVA * $P<0.01$. Closed circles, untreated cells; closed squares, NaHS
479 0.1 mM; closed triangles, NaHS 0.25 mM

480

481 **Figure 4. Exogenous and endogenous H_2S on yeast cells induce ethanol production and ATP**
482 **synthesis.** (A) BY4742 yeast cell cultures were treated with NaHS 0.1 mM and seven hour later
483 supernatants were collected. Ethanol production was measured *in vitro* at 37°C. Closed circles,
484 untreated cells; closed squares, NaHS 0.1 mM. Unpaired t * P=0.04. (B) Yeast cell cultures of the
485 strains BY4741 and BY4742 supernatants were collected at 24 h. Ethanol production was
486 measured *in vitro* at 37°C. Closed squares, BY4741; open squares, BY4742. Unpaired t * P=0.02
487 (C) Yeast cell cultures at exponential phase were treated with NaHS 0.1 and 0.25 mM. Two and
488 four hours later whole cell extracts were lysated and ATP was quantified. ATP production was
489 measure *in vitro* at 37°C. Closed circles, untreated cells; closed squares, NaHS 0.1 mM; closed
490 triangles, NaHS 0.25 mM. One-way ANOVA ** P<0.001.

491

492 **Figure 5. Yeast mutants that accumulate H_2S synthesize ethanol faster and more ATP than**
493 **lower endogenously accumulated H_2S.** (A) 48 hours precultures of yeast cell of the strains *wt*,
494 *met5*Δ*met10*Δ and *met17*Δ were resuspended in fresh media and supernatants were collected every
495 hour. Ethanol production was measured *in vitro* at 37°C. (D) Yeast cell cultures at exponential and
496 stationary phase of the strains *wt*, *met5*Δ*met10*Δ and *met17*Δ were lysated and ATP was quantified.
497 ATP production was measure *in vitro* at 37°C. One-way ANOVA * P<0.05, ** P<0.01. Open
498 circles, *wt*; closed squares, *met5*Δ*met10*Δ; closed diamonds, *met17*Δ.

499

500 **Figure 6. Exogenous H_2S induce ethanol production in *K. marxianus* and *M. guilliermondi*.**
501 (A) *K. marxianus* yeast cell cultures were treated with NaHS 0.1 mM and seven hour later

502 supernatants were collected. Ethanol production was measured *in vitro* at 37°C. Unpaired t **
503 P=0.002. (B) *M. guilliermondi* yeast cell cultures were treated with NaHS 0.1 mM and 24 h later
504 cells were treated again with same concentration of NaHS. Seven hour later supernatants were
505 collected. Ethanol production was measured *in vitro* at 37°C. Unpaired t * P=0.04. Closed circles,
506 untreated cells; closed squares, NaHS 0.1 mM.

507

508 **Supplementary Figure 1. H_2S does not increase the Alcohol dehydrogenase activity two hours**
509 **after stimulation.** Yeast cell cultures at exponential phase were treated with NaHS 0.1 and 0.25
510 mM. Two hours later whole cell extracts were used to measure Alcohol dehydrogenase activity *in*
511 *vitro* at 37°C.

512

Figure 1

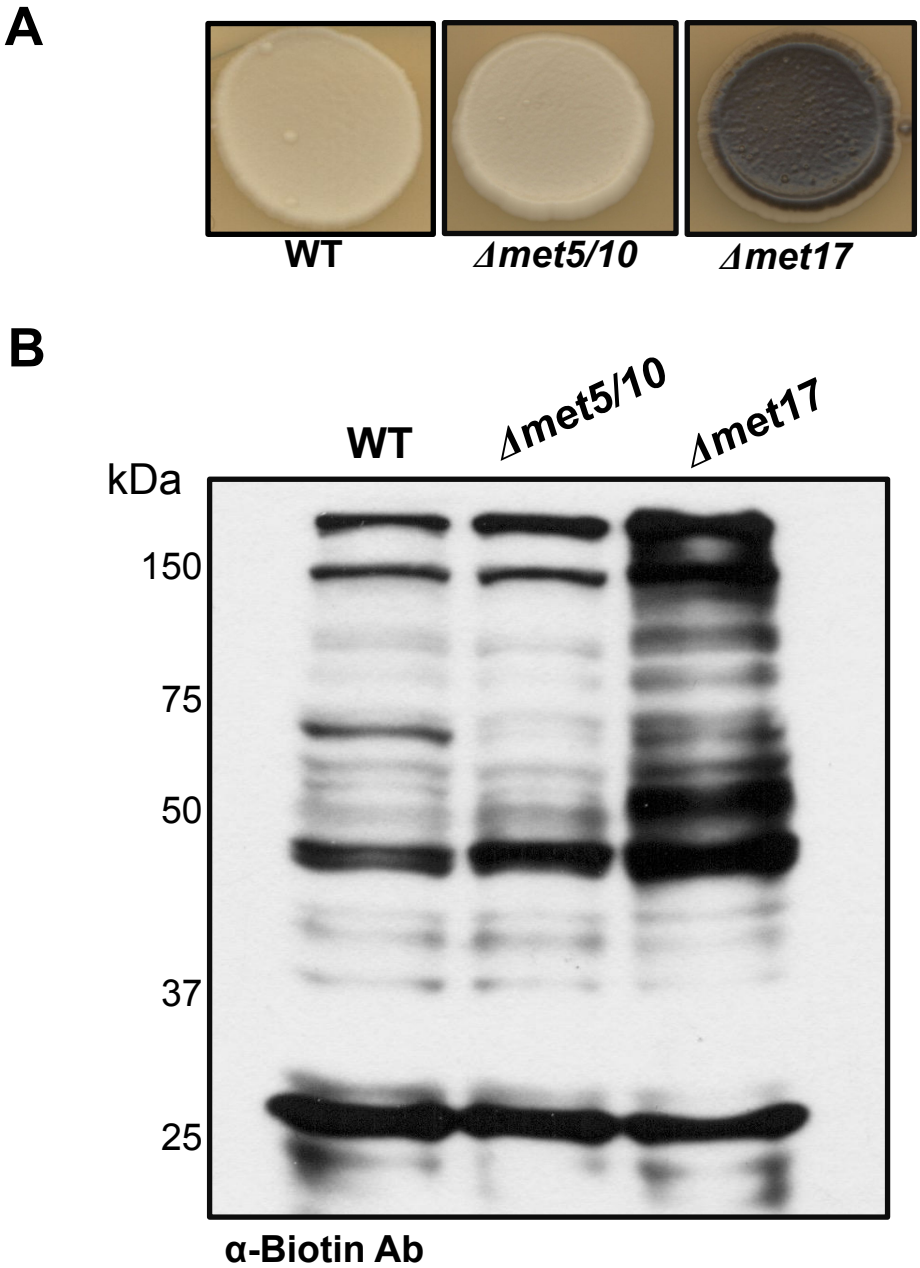
A
WT
Δmet5/10
Δmet17
B
WT
Δmet5/10
Δmet17
kDa
150
75
50
37
25
α-Biotin Ab

Figure 2

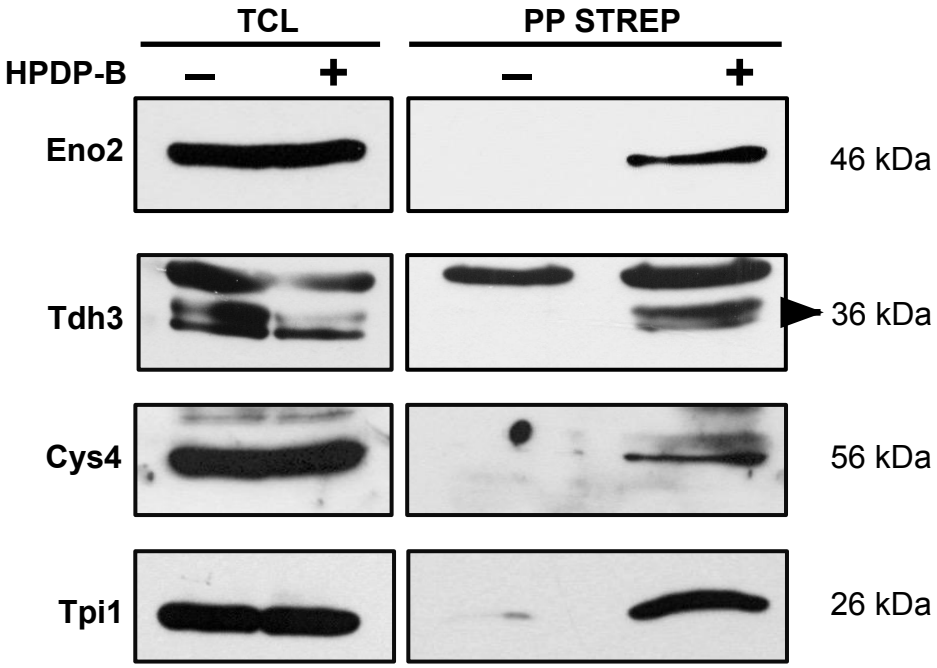
TCL
PP STREP
HPDP-B
–
+
–
+
Eno2
46 kDa
Tdh3
36 kDa
Cys4
56 kDa
Tpi1
26 kDa

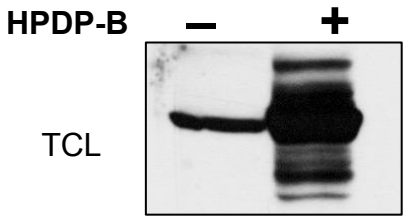
HPDP-B
–
+
TCL

Figure 3

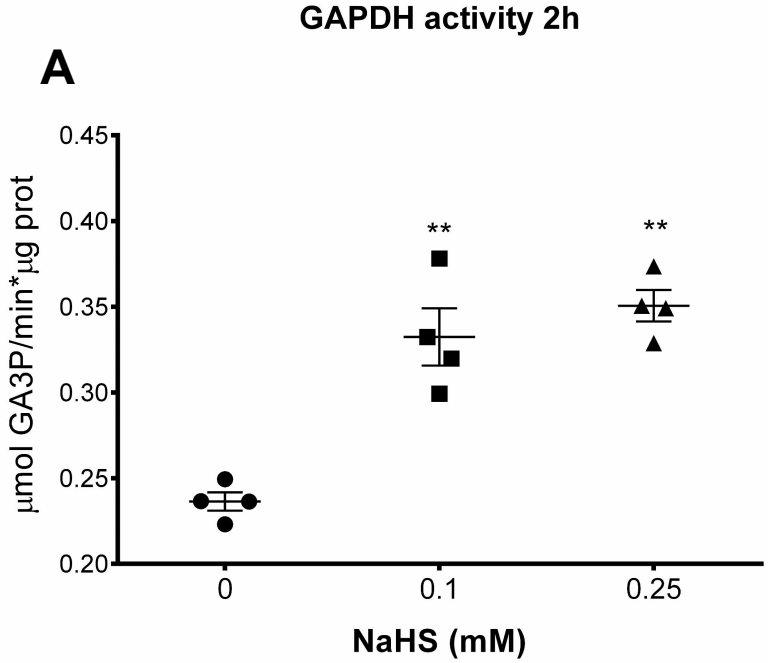
A
GAPDH activity 2h
µmol GA3P/min*µg prot
0.45
0.40
0.35
0.30
0.25
0.20
**
**
0
0.1
0.25
NaHS (mM)

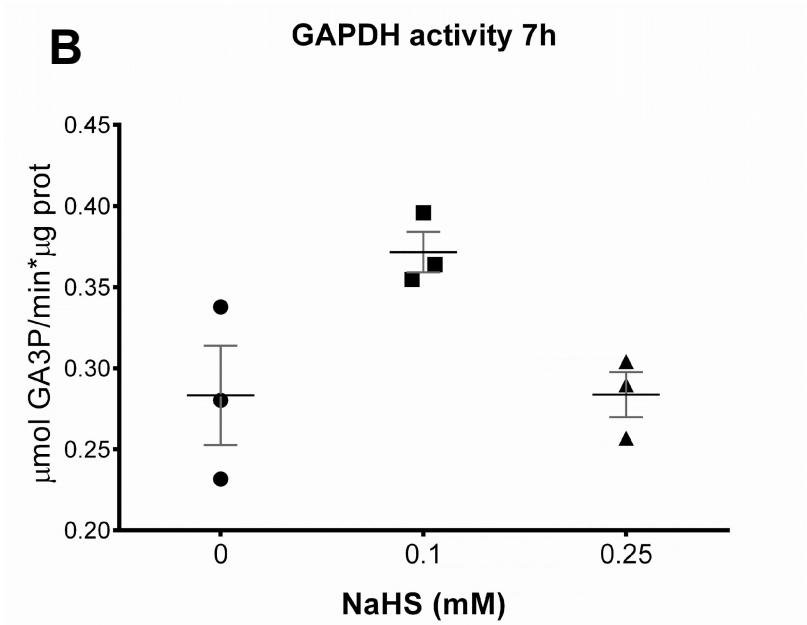
B
GAPDH activity 7h
µmol GA3P/min*µg prot
0.45
0.40
0.35
0.30
0.25
0.20
0
0.1
0.25
NaHS (mM)

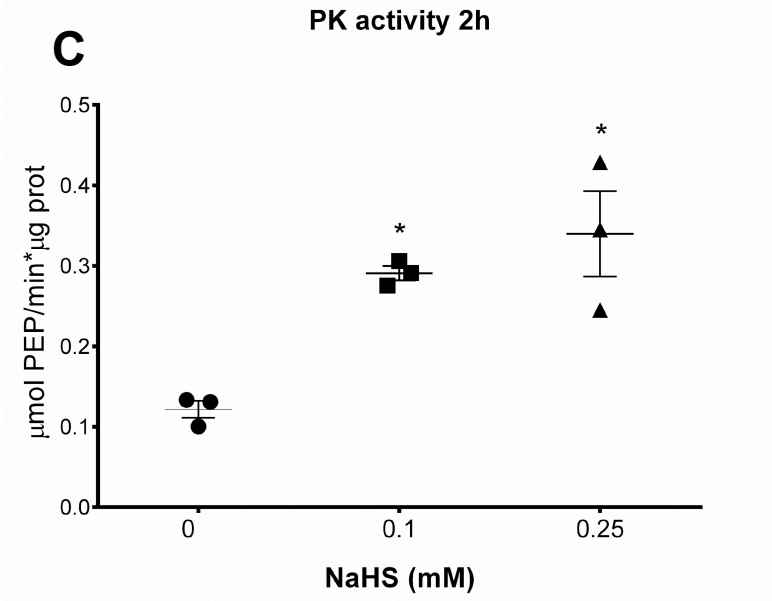
C
PK activity 2h
µmol PEP/min*µg prot
0.5
0.4
0.3
0.2
0.1
0.0
*
*
0
0.1
0.25
NaHS (mM)

Figure 4

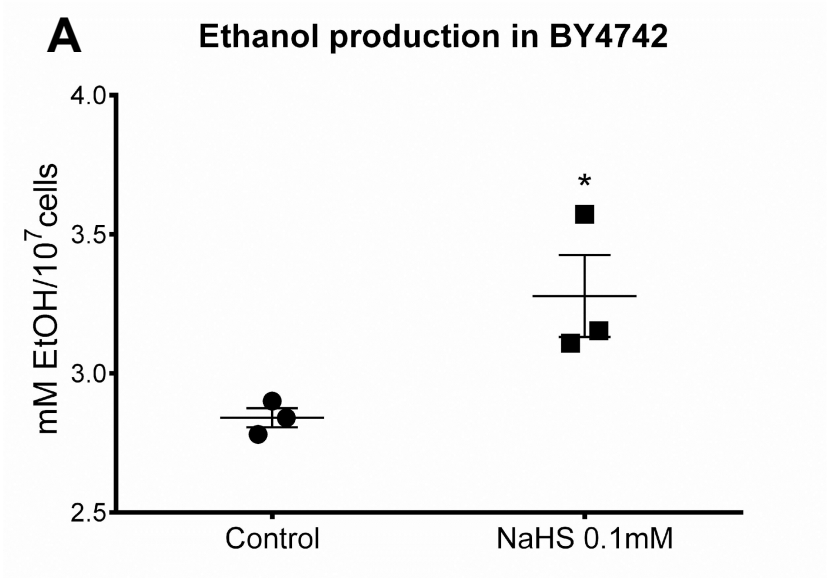
A
Ethanol production in BY4742
mM EtOH/10^7 cells
4.0
3.5
3.0
2.5
*
Control
NaHS 0.1mM

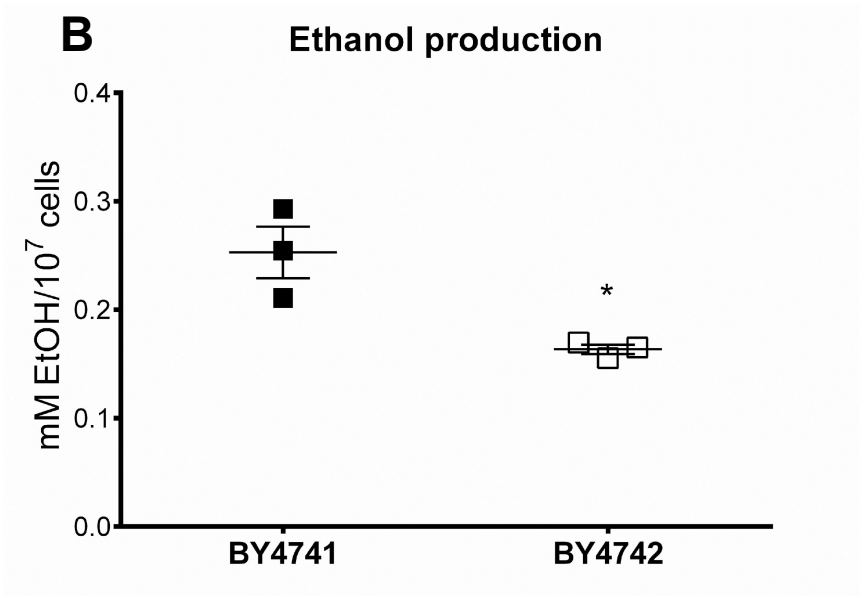
B
Ethanol production
mM EtOH/10^7 cells
0.4
0.3
0.2
0.1
0.0
*
BY4741
BY4742

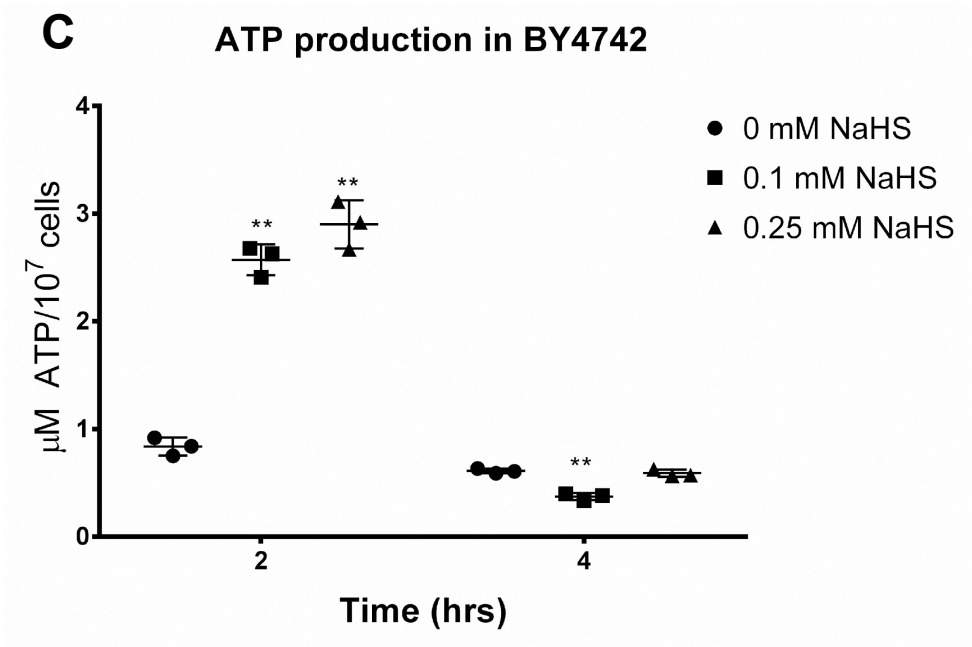
C
ATP production in BY4742
μM ATP/10^7 cells
4
3
2
1
0
**
**
**
2
4
Time (hrs)
0 mM NaHS
0.1 mM NaHS
0.25 mM NaHS

Figure 5

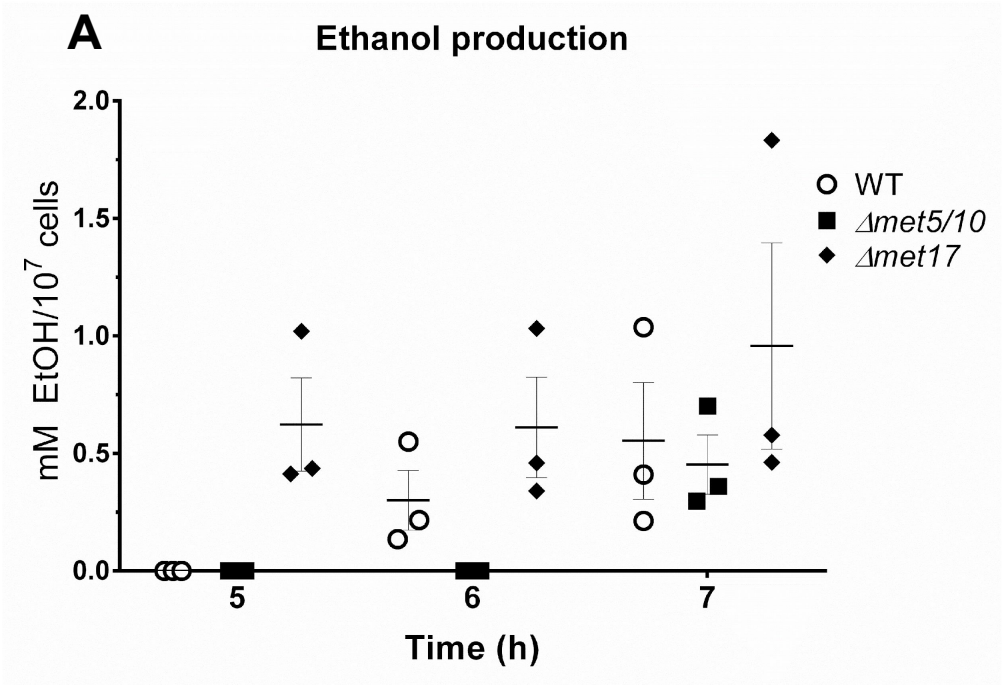
A
Ethanol production
mM EtOH/10^7 cells
2.0
1.5
1.0
0.5
0.0
5
6
7
Time (h)
WT
Δmet5/10
Δmet17

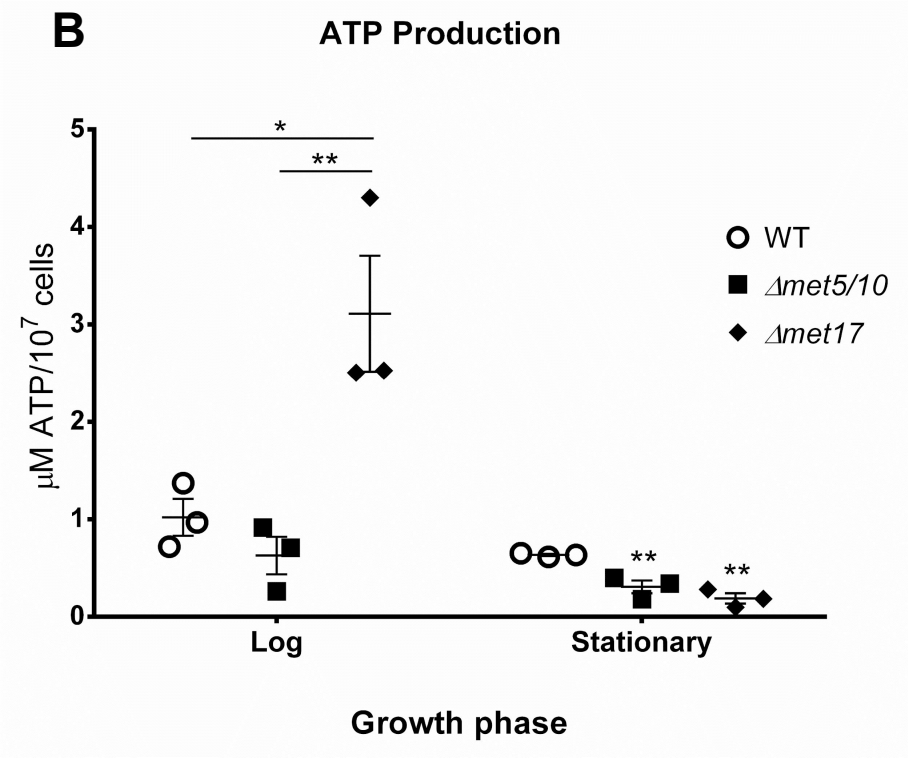
B
ATP Production
μM ATP/10^7 cells
5
4
3
2
1
0
*
**
**
**
Log
Stationary
Growth phase
WT
Δmet5/10
Δmet17

Figure 6

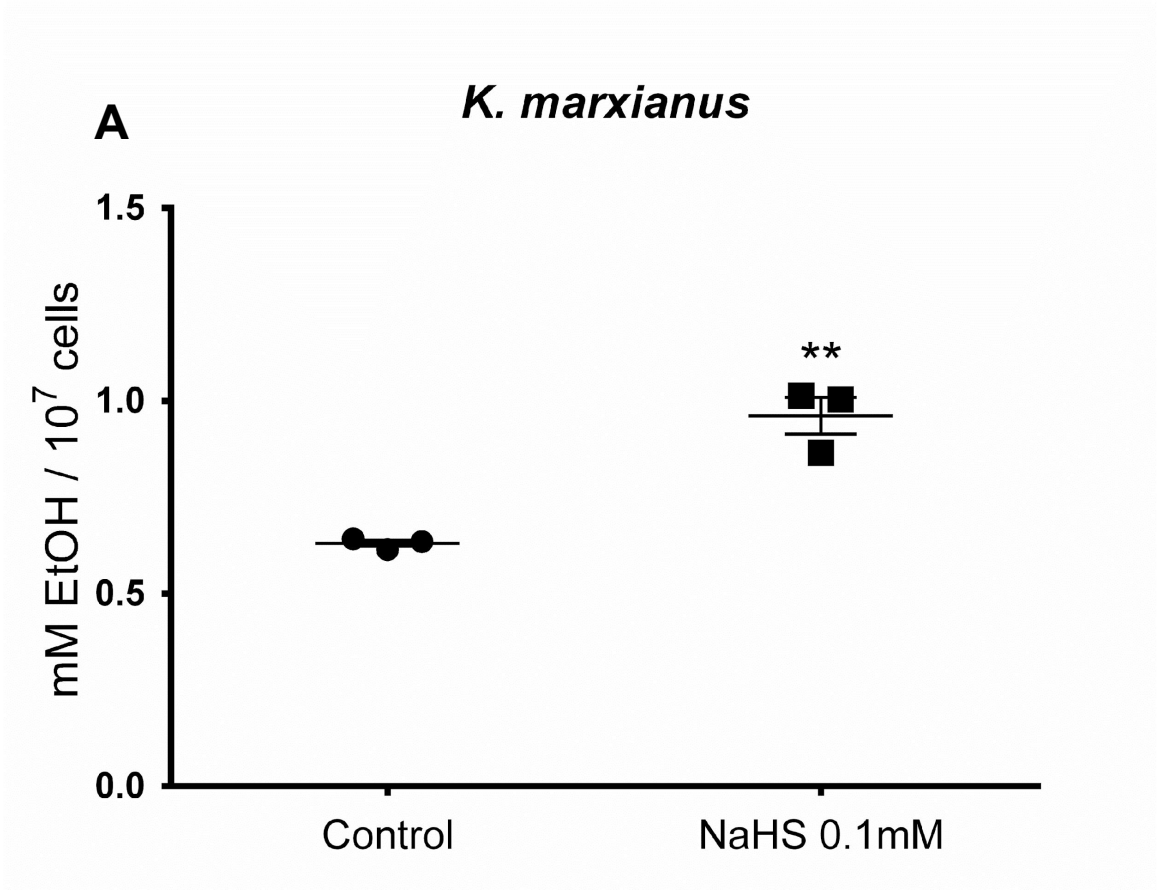
A
K. marxianus
1.5
1.0
0.5
0.0
mM EtOH / 10^7 cells
**
Control
NaHS 0.1mM

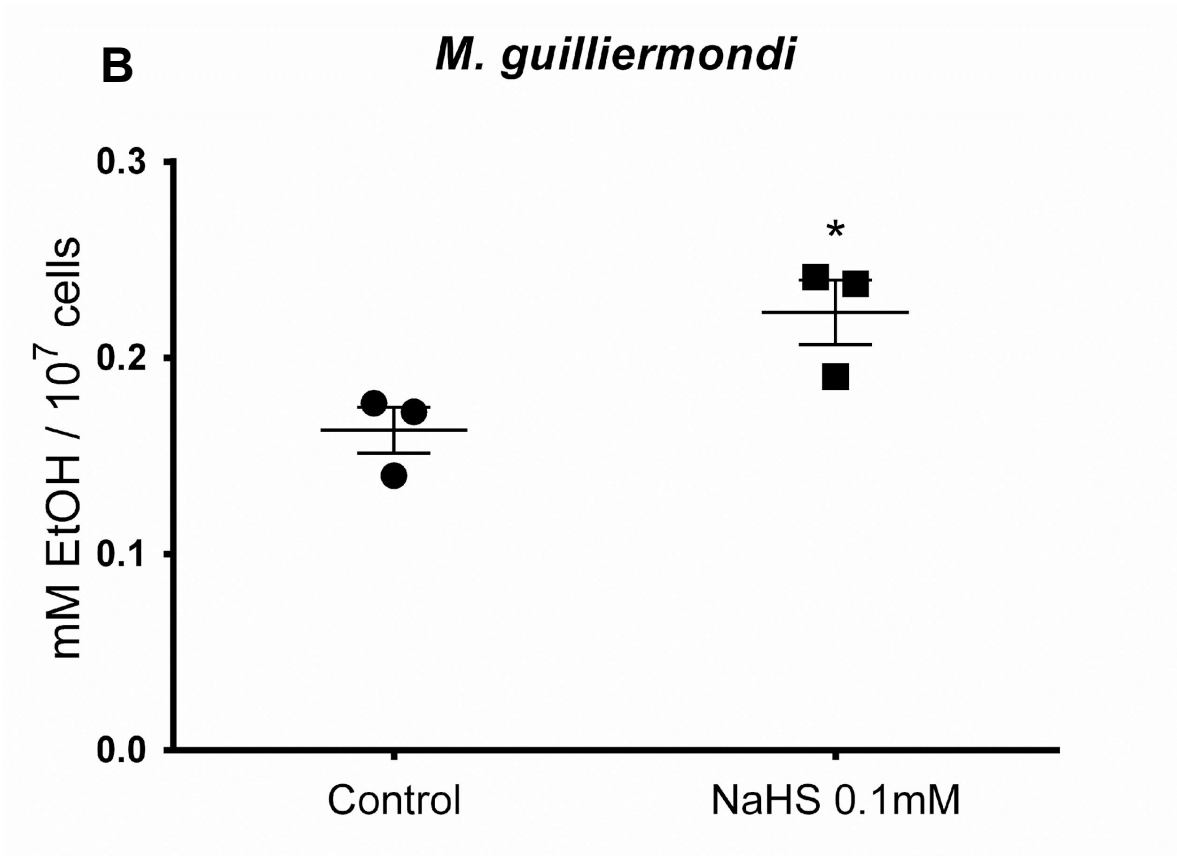
B
M. guilliermondi
0.3
0.2
0.1
0.0
mM EtOH / 10^7 cells
*
Control
NaHS 0.1mM

Supplemental Figure 1

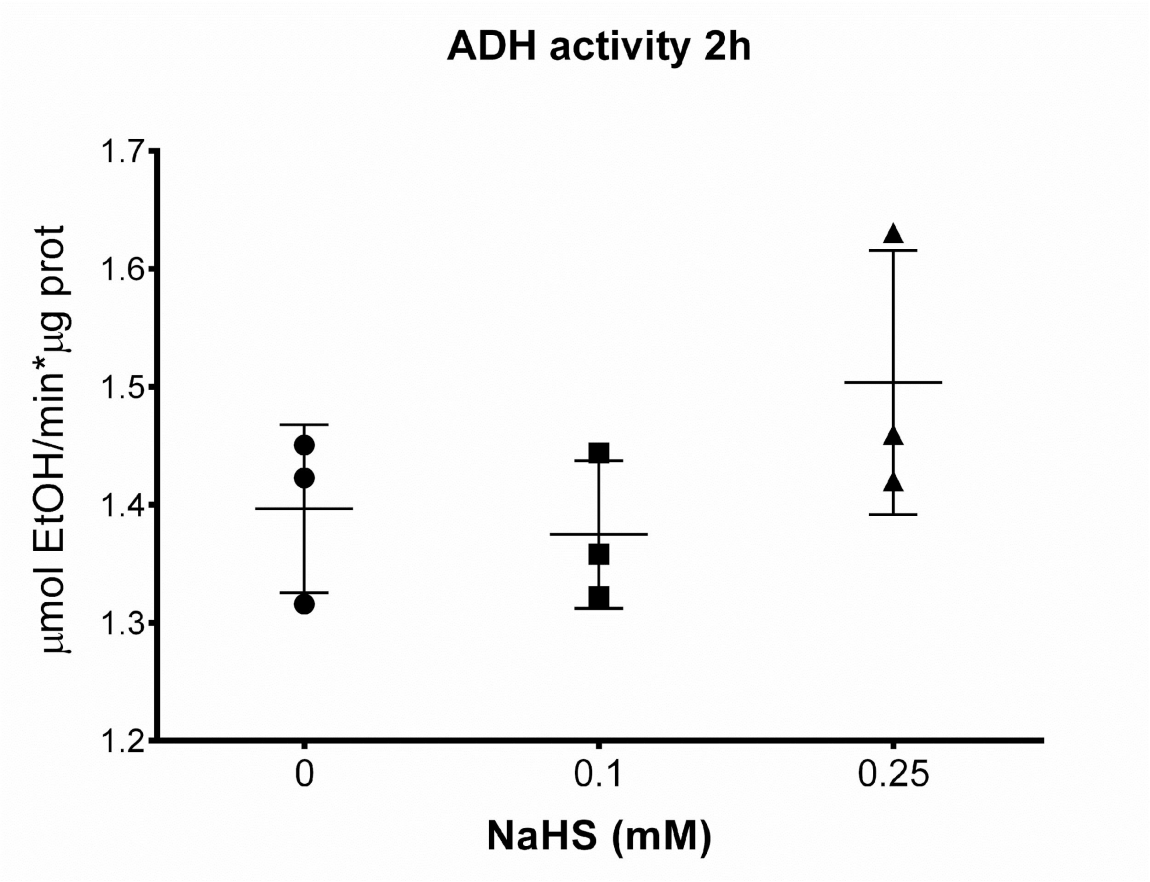

Supplementary Table 1

Yeast strains

Name	Genotype	Source
BY4741	*MAT**a**; his3Δ 1; leu2Δ 0; met15Δ 0; ura3Δ*	Euroscarf
BY4742	*MATα; his3Δ 1; leu2Δ 0; lys2Δ 0; ura3Δ*	Euroscarf
GNO13	*MATα; his3Δ 1; leu2Δ 0; lys2Δ 0; ura3Δ; met5Δ:KanMx; met10Δ:ClonNAT*	This study
PM01	*MATα; his3Δ 1; leu2Δ 0; lys2Δ 0; ura3Δ; met17Δ:KanMx*	This study
Kluyveromyces marxianus	Isolated from mezcal production	Estrada-Ávila 2022
Meyerozyma guilliermondii	Isolated from mezcal production	Estrada- Ávila 2022

Oligonucleotide primers

Name	Secuence
met5F	ATAAAGTAACAGTAGGGAACGGGAACCAGAGAAAAACAAAAGATTGGCGAcagctgaagcttcgtacgc
met5R	AATGTGGGAAGAAAACCCAATAGTATGTCCTACTATGTCATATGCTATCAcataggccactagtggatc
met10F	ATAGTTTTTTTCAACTGCTTTTCCTCGAGGTCACCCAAATATACAACGAGcagctgaagcttcgtacgc
met10R	TTCAAGACAGGTTCAATAAATAGATATTTAGTTTTTATTACTATATTAATcataggccactagtggatc
met17F	TACAGGGTCGTCAGATACATAGATACAATTCTATTACCCCCATCCATACAcagctgaagcttcgtacgc
met17R	TTGTGAGAGAAAGTAGGTTTATACATAATTTTACAACTCATTACGCACACcataggccactagtggatc

Supplementary Table 2

YPGal-Control			
Accession	Protein Name	Unused Score	Coverage (%)
ACAC_YEAST	Acetyl-CoA carboxylase	59.56	44.42
PYC1_YEAST	Pyruvate carboxylase 1	30.46	46.10
SYEC_YEAST	Glutamate--tRNA ligase cytoplasmic	16.73	47.18
ARC1_YEAST	tRNA-aminoacylation cofactor ARC1	10.27	39.10
RS17B_YEAST	40S ribosomal protein S17-B	8.00	75.00
PYC2_YEAST	Pyruvate carboxylase 2	2.00	42.03
YJ41B_YEAST	Transposon Ty4-J Gag-Pol polyprotein	2.00	16.75
RS25B_YEAST	40S ribosomal protein S25-B	2.00	55.56
YPGal- SSH			
Accession	Protein Name	Unused Score	Coverage (%)
ARC1_YEAST	tRNA-aminoacylation cofactor ARC1	18.28	37.23
ADH1_YEAST	Alcohol dehydrogenase 1	14.00	27.01
ALF_YEAST	Fructose-bisphosphate aldolase	12.01	30.36
EF1A_YEAST	Elongation factor 1-alpha	11.53	29.69
ENO2_YEAST	Enolase 2	10.63	47.60
HSP71_YEAST	Heat shock protein SSA1	10.20	40.81
PGK_YEAST	Phosphoglycerate kinase	8.02	37.50
KPYK1_YEAST	Pyruvate kinase 1	8.01	40.00
RL27B_YEAST	60S ribosomal protein L27-B	4.54	38.24
RS3A1_YEAST	40S ribosomal protein S1-A	4.48	38.04
ACAC_YEAST	Acetyl-CoA carboxylase	4.38	15.63
RS8B_YEAST	40S ribosomal protein S8-B	4.15	38.99
TPIS_YEAST	Triosephosphate isomerase	4.13	29.44
RL10_YEAST	60S ribosomal protein L10	4.00	53.39
GAL1_YEAST	Galactokinase	4.00	16.67
G3P3_YEAST	Glyceraldehyde-3-phosphate dehydrogenase 3	4.00	28.92
PDC1_YEAST	Pyruvate decarboxylase isozyme 1	4.00	11.90
PMG1_YEAST	Phosphoglycerate mutase 1	4.00	27.13
RL3_YEAST	60S ribosomal protein L3	2.00	39.02
VDAC1_YEAST	Mitochondrial outer membrane protein porin 1	2.00	32.86
RS4B_YEAST	40S ribosomal protein S4-B	2.00	19.92
RL6A_YEAST	60S ribosomal protein L6-A	2.00	26.70
HSP74_YEAST	Heat shock protein SSA4	1.46	33.02

Supplementary Table 2

YPD-Control			
Accession	Protein Name	Unused Score	Coverage (%)
ACAC_YEAST	Acetyl-CoA carboxylase	132.24	70.67
PYC1_YEAST	Pyruvate carboxylase 1	48.95	70.08
SYEC_YEAST	Glutamate--tRNA ligase cytoplasmic	47.71	70.20
ARC1_YEAST	tRNA-aminoacylation cofactor ARC1	31.70	76.60
DUR1_YEAST	Urea amidolyase	21.94	54.55
RS17B_YEAST	40S ribosomal protein S17-B	14.00	95.59
COPA_YEAST	Coatomer subunit alpha	11.51	46.63
PYC1_YEAST	Pyruvate carboxylase 1	6.35	56.53
RL37A_YEAST	60S ribosomal protein L37-A	4.18	86.36
RL17A_YEAST	60S ribosomal protein L17-A	4.07	81.52
RL37B_YEAST	60S ribosomal protein L37-B	4.01	87.50
RS16B_YEAST	40S ribosomal protein S16-B	3.21	94.41
RL35B_YEAST	60S ribosomal protein L35-B	2.34	71.67
RL43B_YEAST	60S ribosomal protein L43-B	2.13	69.57
RS30B_YEAST	40S ribosomal protein S30-B	2.01	87.30
RS15_YEAST	40S ribosomal protein S15	2.00	57.04
RS19B_YEAST	40S ribosomal protein S19-B	2.00	66.67
IRC5_YEAST	Uncharacterized ATP-dependent helicase IRC5	1.96	32.94
RGT1_YEAST	Glucose transport transcription regulator RGT1	1.42	18.38
RL13B_YEAST	60S ribosomal protein L13-B	1.33	80.40

YPD-SSH			
Accession	Protein Name	Unused Score	Coverage (%)
ARC1_YEAST	tRNA-aminoacylation cofactor ARC1	26.13	67.02
KPYK1_YEAST	Pyruvate kinase 1	24.17	63.40
EF1A_YEAST	Elongation factor 1-alpha	24.03	55.90
ADH1_YEAST	Alcohol dehydrogenase 1	18.61	54.60
ACAC_YEAST	Acetyl-CoA carboxylase	18.51	43.48
ALF_YEAST	Fructose-bisphosphate aldolase	14.03	37.88
ENO2_YEAST	Enolase 2	12.09	55.38
RS11B_YEAST	40S ribosomal protein S11-B	11.05	83.33
HSP71_YEAST	Heat shock protein SSA1	10.59	32.87
G3P3_YEAST	Glyceraldehyde-3-phosphate dehydrogenase 3	8.06	49.10
PGK_YEAST	Phosphoglycerate kinase	8.00	54.09
HSP75_YEAST	Heat shock protein SSB1	6.58	32.79
RL3_YEAST	60S ribosomal protein L3	6.15	60.98
RL27B_YEAST	60S ribosomal protein L27-B	6.10	76.47
RS8B_YEAST	40S ribosomal protein S8-B	6.09	53.50
RS16B_YEAST	40S ribosomal protein S16-B	6.03	70.63
PDC1_YEAST	Pyruvate decarboxylase isozyme 1	6.00	22.56
PST2_YEAST	Protoplast secreted protein 2	6.00	36.36
RL20B_YEAST	60S ribosomal protein L20-B	5.70	56.40
RL6B_YEAST	60S ribosomal protein L6-B	4.80	38.07
RS3_YEAST	40S ribosomal protein S3	4.70	63.33
RS4B_YEAST	40S ribosomal protein S4-	4.63	60.54
EF2_YEAST	Elongation factor 2	4.48	31.71
RL10_YEAST	60S ribosomal protein L10	4.11	44.80
RS3A2_YEAST	40S ribosomal protein S1-B	4.09	52.16

Supplementary Table 2

TKT1_YEAST	Transketolase 1	4.03	31.32
RL4A_YEAST	60S ribosomal protein L4-A	4.00	67.68
PMG1_YEAST	Phosphoglycerate mutase 1	4.00	54.25
RS20_YEAST	40S ribosomal protein S20	4.00	71.07
TPIS_YEAST	Triosephosphate isomerase	4.00	25.81
CYPH_YEAST	Peptidyl-prolyl cis-trans isomerase	4.00	25.31
RL7A_YEAST	60S ribosomal protein L7-A	3.50	72.54
RL13B_YEAST	60S ribosomal protein L13-B	2.89	70.35
RL15B_YEAST	60S ribosomal protein L15-B	2.86	76.47
PYR1_YEAST	Protein URA2	2.50	21.54
RL30_YEAST	60S ribosomal protein L30	2.16	50.48
MPG1_YEAST	Mannose-1-phosphate guanyltransferase	2.11	30.75
RS24B_YEAST	40S ribosomal protein S24-B	2.05	68.15
RS19B_YEAST	40S ribosomal protein S19-B	2.01	64.44
RL6A_YEAST	60S ribosomal protein L6-A	2.00	47.16
CG13_YEAST	G1/S-specific cyclin CLN3	2.00	18.79
YCP4_YEAST	Flavoprotein-like protein YCP4	2.00	34.01
HAL9_YEAST	Halotolerance protein 9	1.34	13.20

Supplementary Table 3

Protein activity values

GAPDH 2 h

NaHS mM	Media ± SD
0	0.2364 ± 0.01
0.1	0.3324 ± 0.03
0.25	0.3505 ± 0.02

GAPDH 7 h

NaHS mM	Media ± SD
0	0.2832 ± 0.05
0.1	0.3716 ± 0.02
0.25	0.2837 ± 0.02

PK 2 h

NaHS mM	Media ± SD
0	0.1216 ± 0.02
0.1	0.2909 ± 0.02
0.25	0.3398 ± 0.09